Moroccan Journal of Chemistry
ISSN: 2351-812X
http://revues.imist.ma/?journal=morjchem&page=login
C. Tcheka & al. / Mor. J. Chem. 9 N°2 (2021) 221-231

Removal of Crystal Violet dye from aqueous solutions using chemically activated carbons by H_3PO_4 activation from corn cobs and Corn roots: kinetic and equilibrium isotherm studies

C. Tcheka[(a)]*, D. Abia[(a,b)], D. Iya-sou[(b)] A. L. Tamgho Tamgue[(a)]

[(a)] Department of Chemistry, Faculty of Science, University of Ngaoundere, Ngaoundere, Cameroon
[(b)] Department of Chemical Engineering, School O Chemical Engineering and Mineral Industries, University of Ngaoundere, Ngaoundere, Cameroon

** Corresponding author:*
ctcheka@yahoo.com
Received 26 July 2020,
Revised 12 Dec 2020,
Accepted 23 Jan 2021

Abstract

In this study, corn cobs and corn roots, agricultural by-products and wastes, were used as precursors for preparation of powder activated carbons (PAC-CC and PAC-CR) by chemical activation with H_3PO_4. Functional groups on the surface of both adsorbents were determined by using ATR−FTIR spectroscopy, while their specific surfaces area were calculated using methylene blue adsorption method. Removal of Crystal Violet (CV) dye from aqueous medium onto both adsorbents was carried out at optimal pH of 10. The pseudo-first order and pseudo-second-order models were used to study adsorption kinetics. The Langmuir and Freundlich, isotherm models were employed to analyze the adsorption isotherm. CV dye molecules-activated carbon surface interaction revealed CV dye's monolayer formation over activated carbon's surface and the involvement of chemisorption, as verified by Langmuir isotherm model and pseudo-second order model, respectively. Langmuir maximum adsorption capacity of PAC-CC and PAC-CR for CV dye were 41.80 mg/g and 35.92 mg/g, respectively. From these results, it can be concluded that the activated carbon prepared from corn cobs or roots as precursor can be used as adsorbent for successful removal of dyes in an aqueous medium.

Keywords: *Corn cobs and roots, Activated carbon, H_3PO_4 activation, Adsorption, Crystal Violet dye*

1. Introduction

Environmental pollution has become a major concern of our society, encouraging the development and improvement of clean-up processes, and also focusing on reducing pollution-source factors [1]. Many industries (textile, agro-food and paper) are heavy consumers of water and use organic dyes (soluble or pigmentary) to dye their products. These dyes are both toxic and responsible for the coloration of the waters thus causing the destruction of life in aquatic places [2]. It is therefore essential to limit environmental pollution by setting up an adapted and less expensive treatment pathway for water purification. Today, there are several methods of treating dye-laden effluents; including clotting and flocculation, biodegradation, chemical oxidation, electrochemical methods and adsorption [3−5]. The technique using the principle of adsorption is the most promising method for the removal of dyes for its efficiency in retaining micro pollutants contained in contaminated water. It has become the analytical method of choice, very effective and simple in its use [6,7]. Several previous works report the use of solid materials (clays, zeolites, activated alumina, sludge, biomasses, agricultural residues, industrial by-products and activated carbon) as adsorbents in water discoloration processes [5,8,9]. During the last years, activated carbons from agricultural by-products and wastes have been widely used as adsorbent for removal of loaded dyes in industrial waste water due to their porous structure, high surface area and adsorption capacity [10,11]. These properties are often improved by physical or chemical activation. Generally the porous carbon manufacturing methods are either based on physical activation which are basically gasification reactions of carbon with steam/CO_2/combination of both or based on the chemically activation methods which include dehydrating agents such as phosphoric acid, sodium hydroxide, potassium hydroxide, zinc chloride [11−13]. H_3PO_4 and $ZnCl_2$ are widely reported to be suitable impregnating agents for biomass based lignocellulose precursors [12−15]. Compared with zinc chloride, H_3PO_4 based activated carbons are commercially preferred for applications in food, pharmaceutical and fine chemicals. Moreover, H_3PO_4 is eco-friendly as it is non-polluting, easy to recover by simply solubilizing the salt of H_3PO_4 in water and can be recycled back into the process [12]. In the present work, corn cobs and corn roots powder were modified using phosphoric acid and powder activated carbons were prepared pyrolysis. It aims to valorize the low-value agricultural byproducts and wastes for preparation of low cost activated carbons for water remediation. The kinetics and equilibrium isotherms of CV dye adsorption on PAC-CC, and PAC-CR are also studied.

2. Materials and methods

2.1. ***Sample collection and purification***

The precursor, corn cobs and corn roots (Figure 1) were collected from Maiborno town in Ngaoundere, Adamawa region, Cameroon. They have been chosen as precursors due to their abundance after corn harvest. They were washed with water to take off impurities and subsequently dried naturally. After this step, the solids were crushed and ground, then washed again with distilled water and dried at moderate temperature until a constant mass was obtained. The solid was sieved using a 0.315 mm mesh sieves. Physicochemical characteristics such as dry matter, moisture and ash content of both precursors were determined and are presented in Table. 1.

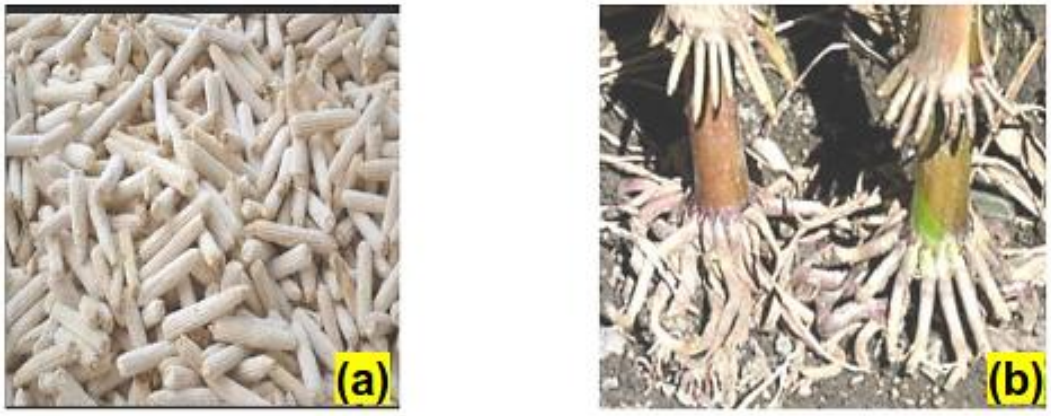

Figure. 1: Photographs of: corn cobs (a), corn roots (b)

Table. 1: Physicochemical characteristics of corn cobs and roots

Sample	Dry matter content (%)	Moisture content (%)	Ash content (%)
CC	88.83± 0.02	11.17± 0.03	23.46± 0.03
CR	87.870± 0.008	12.13± 0.03	8.47± 0.10

*2.2. **Preparation of activated carbon by H_3PO_4 activation***

Phosphoric acid activation was employed in this work to prepare activated carbon according the activation method described by K. Suresh Kumar Reddy and coworkers [12]. The solid obtained as detailed in the above section was utilized as precursor for H_3PO_4 activation. 3.5 g of cobs and roots dust was mixed with 30 mL of 1 N H_3PO_4 (80 %). The mixture was kept at room temperature for 24 h. the paste was obtained and filtered and the solid phase was dried in an oven at 105 °C for 24 h, afterwards, samples were heated to the activation temperature of 550 °C for 90 min using muffle furnace. Finally, upon completion of the experiment, the carbonized samples were cooled in desiccator to the room temperature and washed repetitively with distilled water to remove H_3PO_4. The washed products were then dried in an oven at 105 ºC for 12 h to ensure complete dryness. The sample was crushed and sieved to the desired particle size (< 200 µm).

*2.3. **Characterization of activated carbon samples***

The parameters or properties such as, Iodine Number, Molasses, Tannin, Methylene blue adsorption, Apparent density, Hardness/Abrasion number, Ash contents, Carbon tetrachloride activities, and particle size distribution characterize activated carbon performance. In the present study, the specific surface area of the activated carbons was estimated by using methylene blue adsorption (S_{MB}) and iodine adsorption number (IAN) methods described by Elliot and co-workers [16]. Characterization of functional groups on the surface of PAC-CC and PAC-CR was carried out using a Bruker Alpha FTIR spectrometer with a Diamond Crystal ATR, with spectral range being taken from 4000–500 cm^{-1}. The resolution during spectra registration was fixed at 2 cm^{-1}.

*2.4. **Adsorption experiments***

Adsorption experiments were carried out in batch mode using 200 mL conical flasks containing a total volume of 20 mL of the reaction solution. Reaction mixtures (adsorbent + dye solution) were stirred at constant speed of 350 rpm using magnetic stirrer (MIVAR MAGNETIC STIRRER) for the required time. The effect of several operating

parameters such as, contact time (5−60 min), absorbent dosage (0.01−0.05 g), initial solution pH (2−12), dye concentration (5−30 mg L^{-1}), temperature (299−338 K) on CV adsorption were studied. The initial and residual dye concentrations in aqueous solution were analyzed using a GENESIS-10S-UV−VIS spectrophotometer with wavelength range of 190 −1100 nm, at the wavelengths of maximum absorbance, λ = 595 nm.

The amount of CV adsorbed, (mg g^{-1}) were calculated using the equation 1.

$$q_e = \frac{(C_0 - C_e) \times V}{m} \quad (1)$$

where C_0 and C_e (ppm) are dye concentrations before and after adsorption, respectively, V (L) is the volume of the reaction solution, and m (g) is the mass of adsorbent.

For kinetic experiments, predetermined optimum adsorbent mass of 0.01 g was contacted with 20 mL of CV solution, initial concentration of 20 mg/L. The amount of dye adsorbed at time t (min), q_t (mg g^{-1}), was calculated by equation 2.

$$q_t = \frac{(C_0 - C_t) \times V}{m} \quad (2)$$

where C_t (min) is the dye concentration at a specific time t.

3. Results and discussion

3.1. Adsorbents characterization

3.1.1. Iodine adsorption number (IAN)

Iodine adsorption number is the most fundamental parameter used to characterize activated carbon performance. It is a measure of activity level (Higher degree indicates higher activation), often reported in mg/g. It is a measure of the microspore content of the activated carbon and IAN of a porous carbon should be higher than 900 mg/g [17,18]. According the IAN values of PAC-CC and PAC-CR (1218.28 mg/g and 1675.14 mg/g, respectively) displayed on Table 2, both activated carbons have developed high porosity. However, PAC-CR present high IAN value than PAC-CC. It implies both adsorbents presented high degree of activation and high affinity for small sized contaminants and could also be more susceptible to steric hindrances when sorbates of medium and large sized molecules are involved [17].

3.1.2. Specific surface area (S_{MB})

Some carbon have mesoporous structure which adsorb medium size molecules such as dye Methylene blue. Methylene blue was commonly chosen because of its known strong adsorption onto solids and its recognized usefulness in characterizing adsorptive material. Surface area calculated using methylene blue adsorption method are presented in Table 2. From these results it can be observed that PAC-CC have higher specific surface area than PAC-CR (489.80 and 356.22 m^2/g, respectively). Specific surface area directly related to porosity, high porosity implies high specific surface area. The obtained values in this study are comparable with those reported in the literature (range of 300−1500 m^2/g) [19]. In view of the above values, it can be conclude that PAC-CC and PAC-CR activated using phosphoric acid H_3PO_4 offer high surface area and can be us as potential adsorbent for pollutant up take from aqueous solutions.

Table. 2: IAN and S_{MB} of PAC-CC and PAC-CR.

Adsorbent	IAN (mg/g)	S_{MB} (m^2/g)
PAC-CC	1218.28 ± 0.03	489.80 ± 0.2
PAC-CR	1675.14 ± 0.08	356.22 ± 0.4

3.1.3. ***FTIR Analysis***

The FTIR spectra of PAC-CC and PAC-CR are shown in Figure 2. Various functional groups are observed. At general overview, the vibration peaks for different bonds of functional groups appear almost at the same wavelength number values, which means that the surfaces of both adsorbents presents the same functional groups. Peaks located at 3838 and 3750 cm^{-1} corresponding to (O – H) stretching vibrations of water, alcohol and phenols as possible compounds [12,20,21] The peak observed at 3040 and 3064 cm^{-1}, and another between 987 and 749 cm^{-1} can be attributed to the aliphatic saturated C−H stretching vibrations of in lignin polysaccharides including cellulose and hemicellulose [15,22,]. Two band located at about 1567 and 1578 cm^{-1} on the both adsorbents respectively, could be attributed to the (C = O) weak stretching vibrations in aromatic rings and alkenes [20, 23]. The band observed at 1072 and 1148 cm^{-1} could be ascribed to (−OH) stretching vibrations and (C – O) of phenolic group and aliphatic alcohol [7,10].

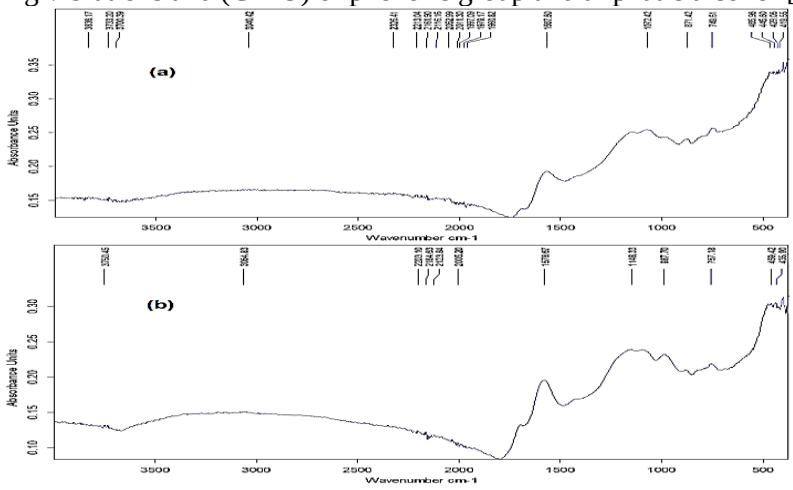

Figure. 1. FTIR spectra of PAC-CC (a) and PAC-CR (b)

3.2. ***Study of cv adsorption***

3.2.1. ***Effect of adsorbent dose***

PAC-CC and PAC-CR quantity influence over the CV removal is presented in Figure 3. It can be seen that as the adsorbent quantity increases, adsorption capacity decreases. The optimum adsorbent quantity was found to be 0.01 g for both adsorbents. The adsorption capacity of PAC-CC was 30.00 mg/g, whereas the adsorption capacity of PAC-CR was 28.87 mg/g. This observation indicated that PAC-CC had a higher CV retention capacity than PAC-CR. Adsorbent quantities higher than 0.01 mg displayed a gradual decrease in q_e. The decrease in q_e at higher dosage is due to a decrease in the number of occupied sites per unit mass [14,24]. Therefore, according to this result all further adsorption experiments were carried out with optimal adsorbent dose values of 0.01 g for PAC-CC and PAC-CR adsorbents.

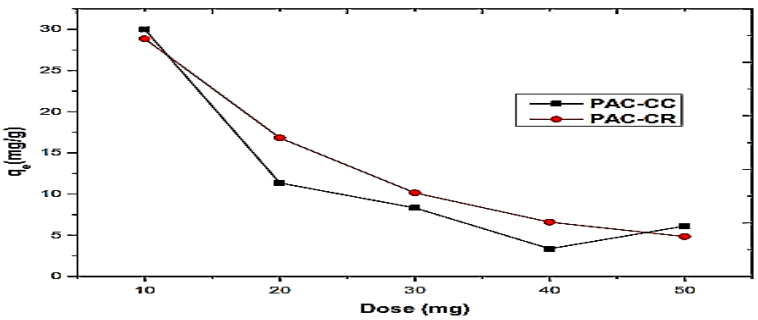

Figure. 3: Effect of adsorbent quantity over CV dye adsorption onto PAC-CC and PAC-CR (C_i = 20 mg L^{-1}; V = 20 mL; T = 25 ± 2 °C; 350 rpm)

3.2.2. ***Effect of pH***

As is reported in several papers [25, 26], adsorption process is reliant on the aqueous phase pH, and the functional groups on the adsorbent, and their ionic states (at particular pH). Effect of solution pH over CV adsorption onto PAC-CC and PAC-CR has been studied on the pH range 2-12 with initial concentration of dye solution of 20 mg/L. Figure 4 shows variation of adsorbed amount onto both adsorbent as function of solution pH. It can be observed that adsorbed amounts decrease when pH increase from 2 to 6, then increase for pH ranging from 6 to 10 and tends to reach the maximum values at pH 10. At extreme pH, acid or basic, the adsorption capacities are high, however, it's is higher at pH 10 than that at pH 6. From this observation, the mechanism of adsorption by attractive electrostatic interactions between the negative charges of the surface of activated carbon and positive charges of CV dye molecules can be considered [27, 28]. The lower adsorption capacity at acid pH (4-6) could be ascribed to the presence of excess H^+ ions competing with the dye cations (CV^+) for the adsorption sites [26]. Further experiments were conducted at pH 10.

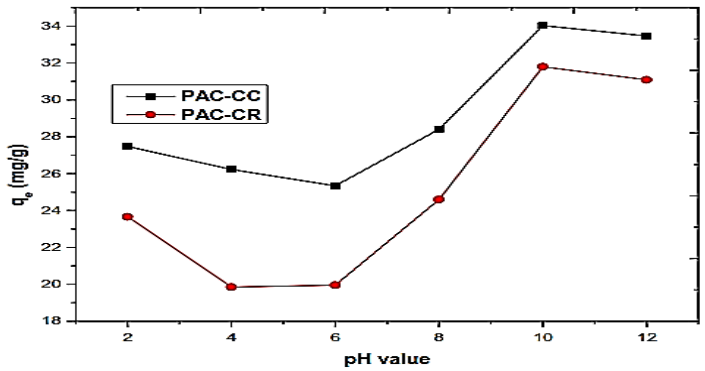

Figure. 4: Effect of pH on CV adsorption capacity (V = 20 mL; m_{PAC} = 0,01g; t = 30 min; T = 25 ± 2; 350 rpm)

3.2.3. ***Effect of contact time and kinetic models***

The evaluation of the effect of contact time is essential because it provides fundamental information on how fast the adsorption process reaches equilibrium. From the results presented in Figure 5, it was observed the fast dye adsorption at initial stage, which became gradually slower as equilibrium was approached. Experimental values of adsorption capacity, $q_{e,exp}$ for adsorption of CV onto both adsorbents at the initial concentration of 20 mg/L were 30.06 mg/g et 24.58 mg/g, respectively .The time required to reach equilibrium was found to be 30 min. Numerous and vacant active surface sites of adsorbent were available in the early stages of the adsorption, while as the contact time increased, the number of vacant sites decreased, thereby slowing down the adsorption process. Similarly, the increase of the initial dye concentration led to higher loading rates of the adsorbate molecule, which was attributed to the enhanced driving force of the concentration gradient to the vacant sites of adsorbent [29-31].

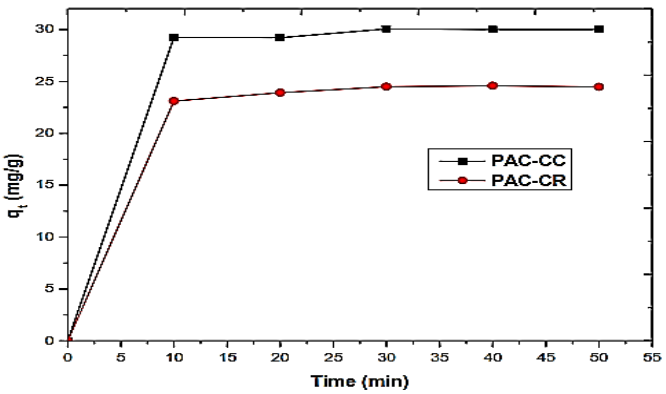

Figure. 5: Effect of contact time over CV adsorption onto PAC-CC and PAC-CR (V = 20 mL; T =25 ± 2 °C; pH = 10; m_{PAC} = 0.01 g; 350 rpm)

The kinetic data were processed using three models: pseudo-first-order, pseudo-second-order, and intra-particle diffusion (Figure 6). The best fit of the experimental data was established based on the value of the coefficient of determination R^2. The linearized form of the pseudo-first-order model deduced from the model established by Lagergren [32] was given by equation 3.

$$\ln(q_e - q_t) = \ln q_e - k_1 \frac{t}{2.303} \quad (3)$$

where q_e and q_t are amount of CV dye per gram of adsorbent (mg/g) at equilibrium and function of time respectively, t is the contact time (min) and k_1 the adsorption rate constant (min^{-1}). The plot of $\ln(q_e - q_t)$ as function of t was used to determine the parameters of the pseudo-first order kinetic model (Table 3**).** The linear equation of the pseudo-second-order kinetic model was given by Ho and McKay [33]:

$$\frac{t}{q_t} = \frac{1}{k_2 q_e^2} + \frac{t}{q_e} \quad (4)$$

where k_2 is the adsorption rate constant (g/mg min). The plot of $\frac{t}{q_t}$ versus t was used to determine the parameters of the pseudo-first-order kinetic model (Table 3). To evaluate the contribution of CV dye diffusion through adsorbent, the rate constant for intra-particle diffusion (k_{id}, mg/(g $min^{1/2}$)) and the intercept C_i (mg/g) were also determined using Weber and Morris model [34] (equation 5).

$$q_t = k_{id} t^{1/2} + C_i \quad (5)$$

Plot of q_t versus $t^{1/2}$ for adsorption of CV dye onto both activated carbons are presented in Figure 6, while the values of k_{id}, C_i and R^2 are represented in Table 3. The regression coefficients (R^2) for different kinetics model for CV adsorption onto PAC-CC and PAC-CR are showed in Table 3. Comparing R^2 values (0.999) for pseudo-second-order, (0.671 and 0.768) for pseudo-first-order and (0.728 and 0.838) for intra-particle diffusion models, it's clear that adsorption of CR over both adsorbents surface follow pseudo-second order kinetics and thus theoretically rate-limiting step would involve chemical interaction i.e. chemisorption [21]. The same can further be verified from the experimental adsorption capacities ($q_{e,\,exp.}$), (30.06 mg/g and 24.58 mg/g) appear to be almost equal to theoretical adsorption capacity ($q_{e,\,cal}$), (30.34 mg/g and 24.93 mg/g) values as predicted by pseudo-second-order model for both CV adsorption on both PAC-CC and PAC-CR.

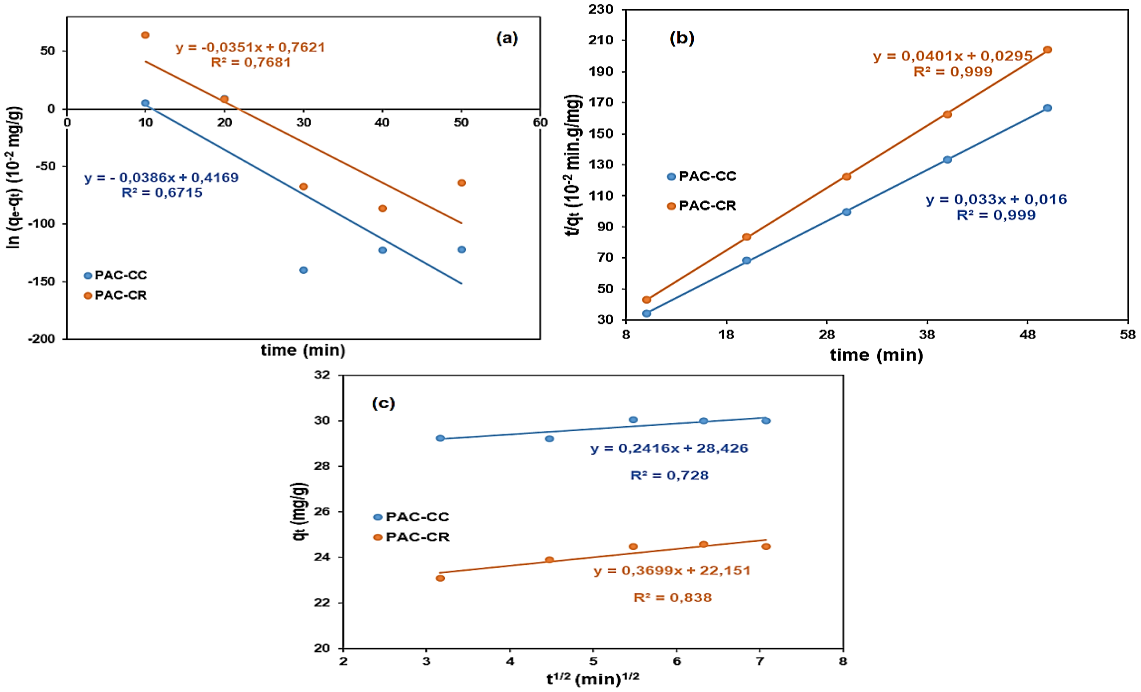

Figure. 6: Pseudo-first-order (a), pseudo-second-order (b), and intra-particle diffusion (c) kinetic models of CV dye adsorption onto PAC-CC and PAC-CR (V = 20 mL; T = 25 ± 2 °C; pH = 10; m_{PAC} = 0.01 g; 350 rpm)

Table. 3. Kinetic parameters for the adsorption of CV molecules onto PAC-CC and PAC-CR at initial concentration of 20 mg/L (V = 100 mL; T = 26 ± 2 °C; pH = 4.17; m_{AC} = 0.01 g; 350 rpm)

Adsorbent	Pseudo-first-order				Pseudo-second-order			Intra-particle diffusion		
	$q_{e,exp}$ (mg/g)	k_1 (min^{-1})	$q_{e,cal}$ (mg/g)	R^2	k_2 (g/(mg.min))	$q_{e,cal}$ (mg/g)	R^2	k_{id} (mg/(g,min)$^{1/2}$))	C_i (mg/g)	R^2
PAC-CC	30.06	0.089	1.52	0.671	0.068	30.34	0.999	0.242	28.426	0.728
PAC-CR	24.58	0.081	2.14	0.768	0.054	24.93	0.999	0.370	22.151	0.838

3.2.4. ***Effect of initial dye concentration and isotherms models***

The initial dye concentration can influence the adsorption capacity of the adsorbent, therefore the next step of the study was to vary the initial CV dye concentration from 10 to 30 mg/L. The residual concentrations were determined and the obtained results are presented in Figure 6.a. From the results obtained it can be observed that PAC-CC has higher adsorption capacity of CV than PAC-CR. The adsorption increased significantly when initial dye concentration increased from 10 to 20 mg/L, and tend to be constant at the initial concentration range (25-30 mg/L). At lower CV concentrations, an increase in CV adsorbed amount is due to high ratio of adsorbent sites to the dye molecules, while at higher CV concentrations, the adsorption capacity remained constant due to the saturation of the adsorbent surface or possible repulsive force between adsorbed layers and remaining bulk molecules [14]. Therefore, according to this experiment the optimal CV initial concentration value of 20 mg/L were selected for PAC-CC and PAC-CR adsorbents, respectively, to carry out the further adsorption experiments. Adsorptions isotherms are important for the description of how molecules of adsorbate interact with the adsorbent surface [26]. Two isotherm models Langmuir [35] and Freundlich [37] were used to describe the adsorption process of CV onto both adsorbents. Langmuir adsorption isotherm describes quantitatively the formation of a monolayer adsorbate on the outer surface of the adsorbent, and after that no further adsorption takes place. Thereby, the Langmuir represents the equilibrium distribution of adsorbate (dye molecules) between the solid and liquid phases [23]. The model assumes uniform energies of adsorption onto the surface and no transmigration of adsorbate in the plane of the surface. The linear forms of the Langmuir (equation 6) adsorption isotherm can be expressed as follows:

$$\frac{C_e}{q_e} = \frac{1}{q_m K_L} + \frac{C_e}{q_m} \quad (6)$$

where C_e (mg/L) is the equilibrium dye concentration, q_m is the maximum monolayer adsorption capacity of the adsorbent (mg/g), and K_L is the Langmuir constant represents the adsorption affinity (L/mg).

The essential features of the Langmuir isotherm, which is a dimensionless constant referred to as separation factor or equilibrium parameter [26].

$$R_L = \frac{1}{1+K_L C_0} \quad (7)$$

where C_0 is the highest initial dye concentration. R_L value indicates the adsorption nature to be either unfavorable (R_L > 1), linear (R_L = 1), favorable (0 < R_L < 1), and irreversible (R_L= 0) [31, 37, 38]

The Freundlich model takes account of multilayer coverage where adsorption is still possible on the adsorbate saturated adsorbent's surface. It is applicable for adsorption on heterogeneous surfaces with uniform energy distribution and reversible adsorption [26]. The linear form of the Freundlich adsorption isotherm (equation 7) can be expressed as follows:

$$\ln q_e = \ln K_F + \frac{1}{n} \ln C_e \quad (7)$$

where, K_F is the Freundlich parameter associated with the adsorption affinity ((mg/g).(mg/L)$^{1/n}$) is the Freundlich constant and taken as indicator of adsorption capacity, and 1/n is a measure of the adsorption intensity. If 1/n = 1, the

adsorption is linear i.e. the adsorption site are homogeneous and there is no interaction between the adsorbed species. If 1/n < 1, the adsorption is favorable; the adsorption capacity increases and new adsorption sites appear. If 1/n > 1, the adsorption is unfavorable; the adsorption bonds become weak and the adsorption capacity decreases [26]

Isotherms model parameters are obtained by determining the slope and intercept or their linear plots (Figures (6.a) and (6.b)) as shown in Table 5. In order to choose the isotherm model that best describes the experimental data; two comparisons were made based on the R^2.

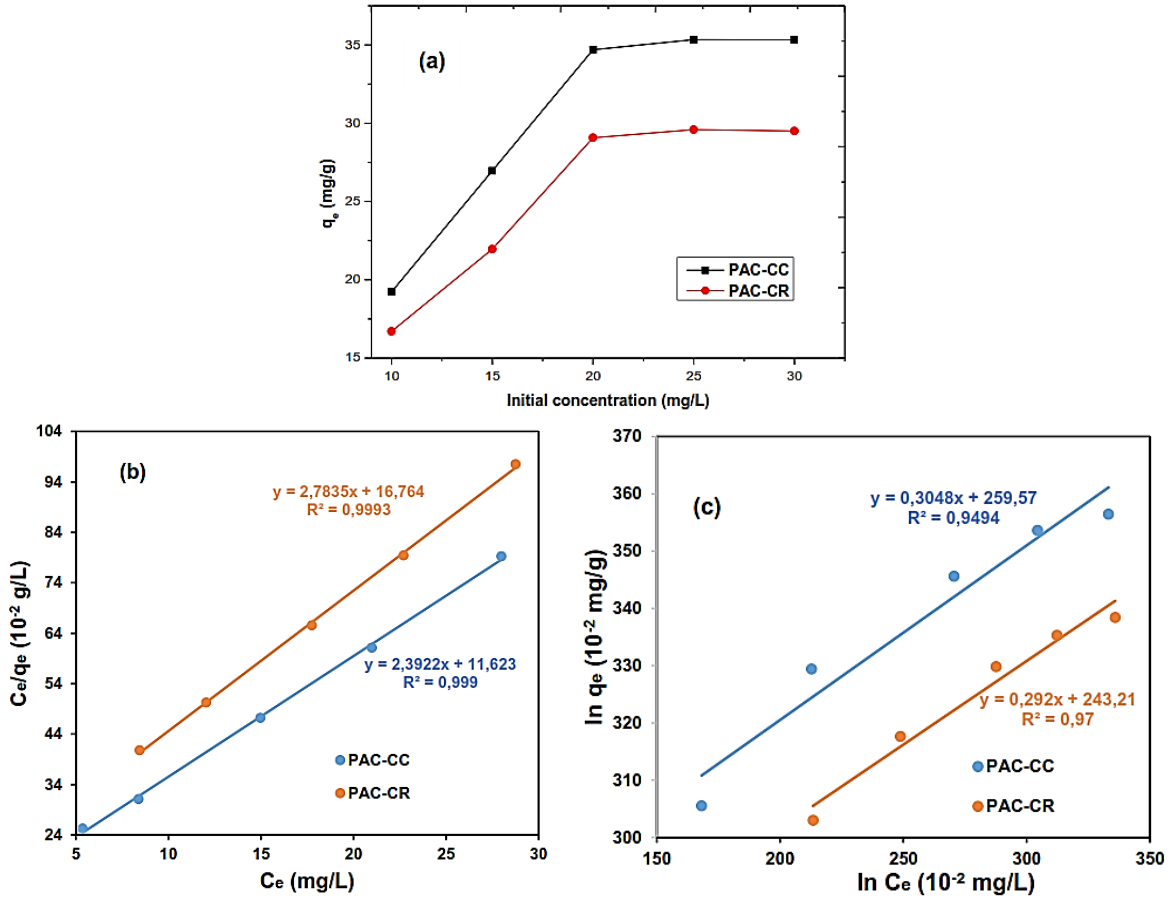

Figure. 6: Effect of initial concentration (a), Equilibrium adsorption isotherms: Langmuir (b), Freundlich (c) models for CV adsorption onto PAC-CC and PAC-CR (V =20mL; T = 25±2°C; pH =10; m_{PAC} = 0.01 g; 350 rpm; t = 30 min)

Comparing the R^2 values, the Langmuir isotherm model has higher value than the Freundlich for both adsorbents, which indicates that Langmuir model was the best fit to the experimental data. Maximum monolayer adsorption capacities of PAC-CC and PAC-CR, q_m, obtained from the Langmuir isotherm model are found as 41.80 mg/g and 35.92 mg/g, respectively, which indicate one more time that PAC-CC has higher adsorption capacity of CV dye than PAC-CR. The values of R_L were between 0 and 1 (0.139 for PAC-CC and 0.167 for PAC-CR) indicating that adsorption was favorable [37, 39]. The relatively high value of Langmuir constant K_L indicate that chemisorption is the predominant mechanism of the CV dye adsorption process [40]. The high values of K_F indicated that both adsorbents have a higher adsorption capacity and affinity for CV dye molecules. The values of 1/n for CV dye adsorption onto both adsorbents less than 1 indicate favorable adsorption [41, 42].

Table. 5: Isotherm parameters obtained for the adsorption of CV dye onto PAC-CC and PAC-CR (C_i = 20 mg/L; V = 20 mL; T =25±2°C; pH = 10; m_{PAC} = 0.5 g; 350 rpm)

Adsorbent	Langmuir				Freundlich		
	q_m (mg/g)	K_L (L/mg)	R_L	R^2	K_F (mg/g).(L/mg)$^{1/n}$	$1/n_F$	R^2
PAC-CC	41.80	0.206	0.139	0.999	13.406	0.305	0.949
PAC-CR	35.92	0.166	0.167	0.999	11.383	0.292	0.970

4. Conclusion

Powder activated carbons (PAC-CC and PAC-CR) from corn cobs and roots prepared by chemical activation with phosphoric acid H_3PO_4 evaluated as potential adsorbents for Crystal Violet dye removal from aqueous solution. Adsorption process parameters were found to affect the adsorption performance of CV using PAC-CC and PAC-CR. The maximum adsorption capacities were 41.80 mg/g (PAC-CC) and 35.92 mg/g (PAC-CR) for CV removal from aqueous medium. The better fittness of equilibrium data with Langmuir isotherm model indicated that CV adsorption onto PAC-CC and PAC-CR occurs through the monolayer formation. The kinetic study and analysis of the adsorption experimental data revealed that the CV adsorption process fitted the pseudo-second-order kinetic model, exemplified chemisorption. These results showed that powder activated carbons from corn cobs and roots, H_3PO_4 activated might be used as adsorbent for treatment of water contaminated with Crystal Violet dye.

5. References

[1] Khalfaoui A., *Thèse de doctorat, Faculté des Sciences, Université de Constantine, Algérie,* (2012) 180.

[2] T.S. Anirudhan, M. Ramachandran, *Process and Environmental Protection*, 95 (2015) 215-225.

[3] M. J. Ahmed, S. K. Dhedan, *Fluid Phase Equilibria*, 317 (2012) 9-14

[4] C. Telegang Chekem, V. Goetz, Y. Richardson, G. Plantard, J. Blin, *Catalysis Today* (2018), doi: 10.1016/j.cattod.2018.12.038

[5] A. Djelad, A. Mokhtar, A. Khelifa, et al., *International Journal of Biological Macromolecules*(2018), doi: 10.1016/j.ijbiomac.2019.08.068

[6] S.R. Shirsath, A.P. Patil, R. Patil, J. B. Naik, P. R. Gogate, S. H. Sonawane, *Ultrasonics Sonochemistry*, 20 (2013) 914-923.

[7] H. Du, J. Cheng, M. Wang, M. Tian, X. Yang, Q. Wang, , *Diamond & Related Materials* (2019), doi:10.1016/j.diamond.2019.107646.

[8] A. Machrouhi, H. Alilou, M. Farnane, S. El Hamidi, M. Sadiq, M. Abdennouri, H. Tounsadi, N. Barka, *Journal of Science: Advanced Materials and Devices*, 4 (2019) 544-553.

[9] A. S. Abdulhameed, A. H. Jawad, A.-T. Mohammad, *Bioresource Technology*, 293 (2019) 122071, doi:10.1016/j.biortech.2019.122071

[10] A. Regti, M. R. Laamari, S.-E. Stiriba, M. El Haddad, *Microchemical Journal*, 130 (2017) 129–136.

[11] N. Byamba-Ochir, W. Shim, M. S. Balathanigaimani, H. Moon, *Applied Surface Science*, 379 (2016) 331–337, doi: 10.1016/j.apsusc.2016.04.082

[12] K. S. Kumar Reddy, A. Al Shoaibi, C. C. Srinivasakannan, *New Carbon Materials*, 27(5) (2012) 344-351, doi: 10.1016/S1872-5805(12)60020-1

[13] S. Uçar, M. Erdem, T. Tay, S. Karagöz, *Applied Surface Science, 255 (2009)* 8890–8896.

[14] S. Agarwal, I. Tyagi, V. K. Gupta, N. Ghasemi, M. Shahivand, M. Ghasemi, *Journal of Molecular Liquids*, 218 (2016) 208–218, .doi: 10.1016/j.molliq.2016.02.073.
[15] H. Saygili, F. Güzel, *Journal of Cleaner Production*, 113 (2016) 995-1004, doi: 10.1016/j.jclepro.2015.12.055.
[16] C. Elliott, T. Colby, H. Iticks, *Chest* 96(3) (1989) 672-674, retrieved on 3/05/2009 from http//enwikipedea.org
[17] A. U. Itodo, F. W. Abdulrahman, L. G. Hassan, S. A. Maigandi, H. U. Itodo, *New York Science Journal*, 3(5) *(*2010) , 25-33.
[18] O. A. Ekpete, A. C. Marcus, V.Osi, *Hindawi Journal of Chemistry, 2017*, doi; 10.1155/2017/8635615.
[19] Sekirifa Mohamed L., *Thèse de doctorat, Faculté des Sciences de l'Ingénieur, UNIVERSITÉ BADJI MOKHTAR-ANNABA, Algérie*, (2013) 115.
[20] A. Kumar, H. M. Jena, *Applied Surface Science, 356 (2015), 753-761*, doi: 10.1016/j.apsusc.2015.08.074.
[21] C. Patra, R. Gupta, D. Bedadeep, S. Narayanasamy, *Environmental Pollution* (2020), doi : 10.1016/j.envpol.2020.115102.
[22] R. Davarnejad, S. Afshar, P. Etehadfar, *Arabian Journal of Chemistry*, (2020) 13, 5463–5473, doi: 10.1016/j.arabjc.2020.03.025.
[23] R. Fabryanty, C. Valencia, F. E. Soetaredjo, J. N. Putro, S. P. Santoso, A. Kurniawan, Y.-H. Ju, S. Ismadji, *Journal of Environmental Chemical Engineering*, doi: 10.1016/j.jece.2017.10.057
[24] C. Tcheka, R. P. Chicinas, A. Maicaneanu et al., *Advancements in Materials*, 2 (2018) 1-16.
[25] R. Mariappan, R. Vairamuthu, A. Ganapathy, *Chinese Journal of Chemical Engineering* 23 (2015) 710–721, doi: 10.1016/j.cjche.2014.05.019.
[26] F. Güzel, H. Saygili, G. A. Saygili, F. Koyuncu, *Journal of Molecular Liquids*, 194 (2014) 130-140, doi: 10.1016/j.molliq.2014.01.018.
[27] K. Chinoune, K. Bentaleb, Z. Bouberka, A. Nadim, U. Maschke, *Applied Clay Science*, 123 (2016) 64-75, doi: 10.1016/j.clay.2016.01.006.
[28] A. Mirza, R. Ahmad, *Groundwater for Sustainable Development*, 11 (2020) 100373, doi: 10.1016/j.gsd.2020.100373.
[29] J. Georgin, G. L. Dotto, M. A. Mazutti, E. L. Foletto, *Journal of Environmental Chemical Engineering*, 4 (2016) 266–275, doi: 10.1016/j.jece.2015.11.018.
[30] L. C. Cotet, A. Maicaneanu, *Sci. Technol*. (2013) 37–41.
[31] M. K. Dahri, M. R. Rahimi Kooh, L. B. L. Lim, *Journal of Environmental Chemical Engineering*, 2 (2014) 1434–1444, doi: 10.1016/j.jece.2014.07.008.
[32] S. Lagergren, *Kungliga Svenska Vetenskapsakad Handl*, (1898) 24:1–39.
[33] Y. S. HO and G. MCKAY, *Institution of Chemical Engineers Trans IChem^{E}*, Vol 76, Part B, May 1998.
[34] J. W .J. Weber, J. C. Morris, *J Sanit Eng Div Proceed Am Soc Civil Eng*, (1963). 89:31–59.
[35] I. Langmuir *J Am Chem Soc*, 38 (1916). 2221-2295.
[36] H. M. F. Freundlich, *J Phys Chem*, 57 (1906) 385-470.
[37] M. Rajabzadeh, H. Aghaie, H. Bahrami, *Arabian Journal of Chemistry*, (2019), doi: 10.1016/j.arabjc.2019.07.006.
[38] L. Lilian, L. Guo, C. Guo, *Journal of Hazardous Materials*, 161 (2009) 126–131, doi:10.1016/j.jhazmat.2008.03.063.
[39] Y. Miyah, H. Taouda, A. Lahrichi et al., Journal of the Association of Arab Universities for Basic and Applied Sciences (2019)6), doi: 10.1016/j.jaubas.2016.06.001.
[40] S. Rangabhashiyam, P. Balasubramanian, *Biteb*, (2018), doi:10.1016/j.biteb.2018.06.004
[41] R. Davarnejad, S. Afshar, P. Etehadfar, *Arabian Journal of Chemistry*, 13 (2020) 5463–5473, doi: 10.1016/j.arabjc.2020.03.025
[42] H. R. Ahmed, S. Jassim R., B. K. Aziz, *Karbala International Journal of Modern Science*, (2017) 1-11, doi: 10.1016/j.kijoms.2017.05.002.